DYNAMIC MODEL OF CEMENT PRECALCINATION PROCESS

Zhuo Wang[a, b], Mingzhe Yuan[a], Bin Wang[a], Hong Wang[a], Tianran Wang[a]
[a] Shenyang Institute of Automation of the Chinese Academy of Sciences, Shenyang, Liaoning Province, China
[b] Graduate School of the Chinese Academy of Sciences, Beijing, China
zwang@sia.cn

ABSTRACT
A first principle model of cement precalcination system is developed for the purpose of controller's design and synthesis. The dynamic model is based on the mass and energy balance principle and consists of a set of ordinary differential equations. Based on some logical assumptions, the model not only considers the reaction mechanisms but also reduces the complexity of precalciner system. The model is divided into a preheater submodel and a calciner submodel. Separate submodel for preheater and calciner are initially developed and coupled together to build an integrated model. The model takes the gas content into account and can obtain the values of all key output variables in precalcination process. A stationary solution for the model is found and dynamic simulations of step changes in the input variables are shown.

KEY WORDS
Dynamic model, simulation, precalcination, cement

1. Introduction

At the present time dry process cement production has already become the most advanced technology, and some 80% of the global cement clinker production is obtained from this technology[1]. Control of precalcination in cement production is of great importance because the degree of precalcination of the raw meal affects the quality of the clinker and the operation and the energy requirements of the rotary kiln. Furthermore, fluctuations of the degree of precalcination may cause instability in the whole cement pyroprocess as well as increased carbon monoxide production which is a significant pollution factor that under certain circumstances may lead to explosive gas mixtures[2].

In recent years control problems of this field have attracted more and more attention. Koumboulis *et al.* have provided an indirect adaptive neural controller that regulates the abgasses temperature to control the precalcination degree. The parameters of the controller are computed on the basis of a polynomial neural network that identifies off-line the variations of the real industrial measurements of the variables of the process[3]. Zou *et al.* have respectively proposed the predictive control arithmetics based on the different predictive model to control the calciner temperature, one is the dynamic fuzzy model and the other is grey model[4][5]. Xu *et al.* have proposed a hierarchical composite structure to control the calciner temperature. The algorithm consists of a parameter self-learning PID controller using liner neuron and a feedforward controller and a proportional controller[6]. The literatures cited above have a common ground that they are all based on the "black box" model to design the controller. The "black box" model founded on the experimental data is relatively simple, but it does not find out the relationship of the input and output variables adequately.

The first principle model can understand the reaction mechanisms in the precalciner system and obtain the coupling relationship among the variables. Fidaros *et al.* presented a numerical model and a parametric study of the flow and transport processes taking place in cement calciner. The numerical model is based on the solution of the Navier-Stokes equations for the gas flow, and on Lagrangean dynamics for the discrete particles[7]. But the mathematical models were developed with computational fluid dynamics method and very complicated to design the controller.

The purpose of this paper is to develop a simple first principle model description of cement precalcination process for control purposes. The dynamic properties of this model will be validated and simulated, against the experimental data. Ultimately this work aims at the development of the strategy for control of cement precalcination process.

In the following section a brief introduction to the system is provided and section 3 gives the detailed model formulation of the precalciner system. Section 4 discusses the model validation and shows dynamic simulations of the model.

2. Process Description

The precalciner system investigated here is sketched on Fig. 1. It consists of four-stage cyclone preheater (CP) and a calciner. The calcineous raw meal is passed through the former three preheater before it is sent to the calciner. The operation is similar to that of counter-current heat exchangers and the raw meal is preheated to around calcination temperature by hot gases coming from the calciner. The calcinations of raw meal starts in the calciner once the calcination temperature is reached.

Energy required for the calcination reaction is given by pulverized coal combustion. The tertiary air supplies oxygen for the combustion. The function of the last stage preheater is similar to that of a conventional cyclone separator. The gas reverses its direction and leaves through the exit duct while the solids leave from the bottom to the rotary kiln.

In the precalciner system, manipulated variables are the coal flow rate and the tertiary air flow rate. But the latter does not be adjusted frequently because the tertiary air has strongly coupled with the gas into rotary kiln. The mass flow rate and $CaCO_3$ content of raw meal are the primary disturbances. Because the precalcination rate can not be measured on-line, the gas temperature at the exit of calciner can be considered as the controlled variable. The CP1 exit temperature and the content of O_2 and CO are also the key measured variables.

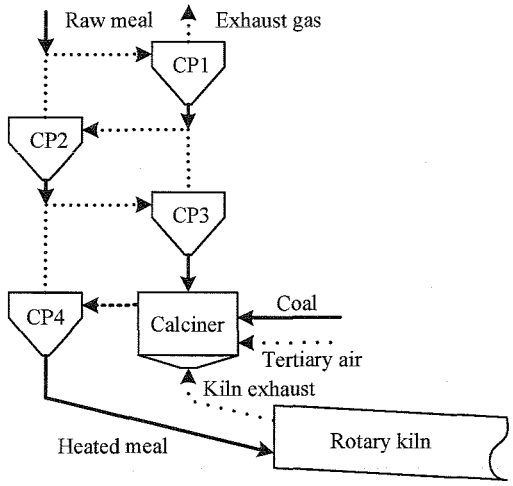

Figure 1. The precalciner system

3. Dynamic Mathematical Model

In developing the model, every effort is made to make it as simple as possible while maintaining the essential dynamics that have been observed qualitatively. Some of assumptions could be relaxed without increasing the computational complexity.

The assumptions which are made are as follows:

- The calcination reaction is assumed to occur only in the calciner.
- Chemical reaction rate follows the Arrhenius law, and secondary reactions were discarded.
- It is supposed that specific heat and reaction heat are constant and temperature independent.
- In every preheater and calciner heat transfer between gas and solid is complete.
- The separate rate of the preheater is constant and determined by the equipment.
- The wall of preheater and calciner is treated as perfect insulator, and the heat loss and air leak are negligible.
- Gas and solid have a completely heat exchange and obtain the same temperature in the heat exchange pipe of preheater.
- Gas, solid and pulverized coal have well-proportioned mixing, and the pulverized coal combusts completely.

The dynamic mathematical model developed includes a set of the heat and mass balance equations. Because the raw meal mainly undergoes the preheated and calcined processes in the precalcination process, the system model can be divided into two submodels, the preheater submodel and the calciner submodel.

3.1 The Preheater Submodel

A schematic of preheater unit considered is shown in Fig. 2. For the dry process, the moisture content is generally present in very small amount (typically ~ 0.5%). The energy requirements for removing the moisture from the raw meal being small (less than 0.5% of the total energy consumption), the raw meal is considered to be free of moisture in this work. However , the developed framework is quite general and including evaporation of moisture is straightforward[8].

There are two types of the raw meal in the preheater, one is the solid leaving from the bottom to the next unit, the other is the entrained solid (dust). The temperature of dust is the same to that of the outflow gas.

Each stage preheater unit consists of a cyclone separator and a heat exchange pipe. The cyclone separator is used to separate solid from gas. And the heat exchange of the gas and solid mainly occurs inside the pipe. Based on the assumption the temperature of mixture can be calculated as follows:

$$T_i = \frac{c_s \cdot f_{s,i-1} \cdot T_{s,i-1} + \left(c_s \cdot f_{d,i+1} + c_g \cdot f_{g,i+1}\right) \cdot T_{g,i+1}}{c_s \cdot \left(f_{s,i-1} + f_{d,i+1}\right) + c_g \cdot f_{g,i+1}} \qquad (1)$$

As can be seen from Fig. 2(b), the input of CP4 differs from the former preheater. Its input is the output of calciner, not the upper preheater output. Therefore the model equations are also different from the former preheater models.

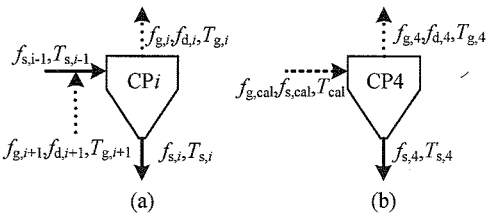

Figure 2. Schematic of (a) preheater 1~3, (b)preheater 4

The balance equations of the preheater submodel are shown in Table 1.

3.2 The Calciner Submodel

The mathematical model of calciner is based on a schematic shown in Fig. 3.

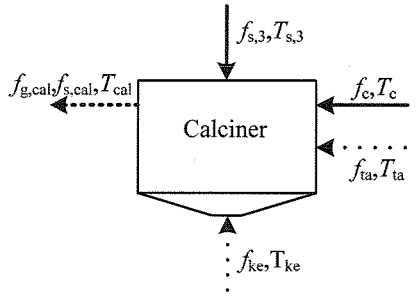

Figure 3. Schematic of calciner

The input streams of calciner are: the preheated raw meal leaving from CP3, the pulverized coal, the tertiary air and the kiln exhaust. The output stream of calciner is the mixture of gas and solid.

As can be seen from the Table 2, the main physicochemical processes taking place in the calciner are coal combustion and the strongly endothermic calcination reaction of the raw meal[9][10].

The reaction rate of calcination and combustion reactions are as follows:

$$r_{CaCO_3} = k_{CaCO_3} \cdot \exp\left(-\frac{E_{CaCO_3}}{R \cdot T_{cal}}\right) \cdot \frac{m_{CaCO_3}}{M_{CaCO_3} \cdot V} \tag{2}$$

$$r_C = k_C \exp\left(-\frac{E_C}{R \cdot T_{cal}}\right) \cdot \frac{m_C}{M_C \cdot V} \cdot \frac{m_{O_2}}{M_{O_2} \cdot V} \tag{3}$$

$$r_{CO} = k_{CO} \exp\left(-\frac{E_{CO}}{R \cdot T_{cal}}\right) \cdot \frac{m_{CO}}{M_{CO} \cdot V} \cdot \frac{m_{O_2}}{M_{O_2} \cdot V} \tag{4}$$

The detailed model equations of calciner are shown in Table 3.

Table 1

Equation system for the preheater submodel (i = 1,2,3)

Mass balance for the gas	$\frac{dm_{g,i}}{dt} = f_{g,i+1} - f_{g,i}$	(5a)
	$\frac{dm_{g,4}}{dt} = f_{g,cal} - f_{g,4}$	(5b)
Mass balance for the dust	$\frac{dm_{d,i}}{dt} = (1-\eta_i) \cdot (f_{s,i-1} + f_{d,i+1}) - f_{d,i}$	(6a)
	$\frac{dm_{d,4}}{dt} = (1-\eta_4) \cdot f_{s,cal} - f_{d,4}$	(6b)
Mass balance for the solid	$\frac{dm_{s,i}}{dt} = \eta_i \cdot (f_{s,i-1} + f_{d,i+1}) - f_{s,i}$	(7a)
	$\frac{dm_{s,4}}{dt} = \eta_4 \cdot f_{s,cal} - f_{s,4}$	(7b)
Energy balance for the gas and dust	$\frac{dT_{g,i}}{dt} = \frac{\left[c_s \cdot (1-\eta_i) \cdot (f_{s,i-1} + f_{d,i+1}) + c_g \cdot f_{g,i+1}\right] \cdot (T_i - T_{g,i})}{(c_g \cdot m_{g,i} + c_s \cdot m_{d,i})}$	(8a)
	$\frac{dT_{g,4}}{dt} = \frac{\left[c_s \cdot (1-\eta_i) \cdot f_{s,cal} + c_g \cdot f_{g,cal}\right] \cdot (T_{cal} - T_{g,4})}{(c_g \cdot m_{g,4} + c_s \cdot m_{d,4})}$	(8b)
Energy balance for the solid	$\frac{dT_{s,i}}{dt} = \frac{c_s \cdot \eta_i \cdot (f_{s,i-1} + f_{d,i+1}) \cdot (T_i - T_{s,i})}{c_s \cdot m_{s,i}}$	(9a)
	$\frac{dT_{s,i}}{dt} = \frac{c_s \cdot \eta_i \cdot (f_{s,i-1} + f_{d,i+1}) \cdot (T_i - T_{s,i})}{c_s \cdot m_{s,i}}$	(9b)

Table 2

Reactions, Kinetics, and Heats of Reactions

Reactions	K_0	E(kJ/mol)	H(kJ/mol)
$CaCO_3 = CaO + CO_2$	1.18×10^3(kmol/m^2·s)	185	179.4
$3C + 2O_2 = CO_2 + 2CO$	1.225×10^7(m/s)	99.77	392.92
$2CO + O_2 = 2CO_2$	3.25×10^7(m/s)	133.8	284.24

Table 3

Equation system for the calciner submodel

Mass balance for the gas	$\frac{dm_g}{dt} = f_{ta} + f_{ke} - f_{g,cal} + \left(r_{CO_2} \cdot M_{CO_2} - r_{O_2} \cdot M_{O_2}\right) \cdot V$	(10)
Mass balance for the solid	$\frac{dm_s}{dt} = f_{s,A} - f_{s,cal} + \left(r_{CaO} \cdot M_{CaO} - r_{CaCO_3} \cdot M_{CaCO_3}\right) \cdot V$	(11)
Component balance	$\frac{dm_{O_2}}{dt} = f_{ke} \cdot p_{O_2,ke} + f_{ta} \cdot p_{O_2,ta} - f_{g,cal} \cdot p_{O_2} - r_{O_2} \cdot M_{O_2} \cdot V$	(12)
	$\frac{dm_{CO_2}}{dt} = f_{ke} \cdot p_{CO_2,ke} + f_{ta} \cdot p_{CO_2,ta} - f_{g,cal} \cdot p_{CO_2} + r_{CO_2} \cdot M_{CO_2} \cdot V$	(13)
	$\frac{dm_{CaCO_3}}{dt} = f_{s,A} \cdot p_{CaCO_3,rm} - f_{CaCO_3,cal} - r_{CaCO_3} \cdot M_{CaCO_3} \cdot V$	(14)
	$\frac{dm_{CaO}}{dt} = -f_{CaO,cal} + r_{CaO} \cdot M_{CaO} \cdot V$	(15)
	$\frac{dm_{Fe_2O_3}}{dt} = f_{s,A} \cdot p_{Fe_2O_3,rm} - f_{Fe_2O_3,cal}$	(16)
	$\frac{dm_{Al_2O_3}}{dt} = f_{s,A} \cdot p_{Al_2O_3,rm} - f_{Al_2O_3,cal}$	(17)
	$\frac{dm_C}{dt} = f_C - r_C \cdot M_C \cdot V$	(18)
Energy balance for the mixture	$\frac{d\left(c_s \cdot m_s + c_g \cdot m_g + c_C \cdot m_C\right) \cdot T_{cal}}{dt} = c_C \cdot f_C \cdot T_C + c_g \cdot \left(f_{ke} \cdot T_{ke} + f_{ta} \cdot T_{ta}\right) + c_s \cdot f_{s,A} \cdot T_{s,A} - c_g \cdot f_{g,cal} \cdot T_{cal} - c_s \cdot f_{s,cal} \cdot T_{cal} + r_C \cdot M_C \cdot V \cdot \Delta H_C - r_{CaCO_3} \cdot M_{CaCO_3} \cdot V \cdot \Delta H_{CaCO_3}$	(19)

Table 4

The comparison of experimental data and simulation data

	The CP1 exit temperature (K)	The calciner exit temperature (K)	The precalcination rate (%)	The O2 content (%)	The CO content (%)
experimental data	612	1148	91.3	2.80	0.1
simulation data	616	1154	92.1	2.81	0.15

4. Process Simulations

The process model has been implemented and simulated in MATLAB®. The validation data are from the hot experiment of cement plant[2]. Under the same conditions, the values of the key output variables are shown in Table 4. Given the precalciner system in the steady state operation some step changes have been simulated in the input variables in order to investigate the dynamic behavior. The open-loop process response for the key output variable is evaluated.

4.1 Change in The Mass Flow Rate of Raw Meal

The mass flow rate of raw meal is one of the main disturbance variables, therefore a step change of magnitude +10% has been applied after 100s simulation and the actuator is again given its initial value after the transient has settled. The obtained results are shown in Fig. 4.

When the mass flow rate of raw meal is augmented, an appreciable drop of the gas temperature at the CP1 and calciner exit is observed. The precalcination rate also has a decrease, while the O_2 content has an increase. The required time to reach the new steady-state operating point is approximate 200s.

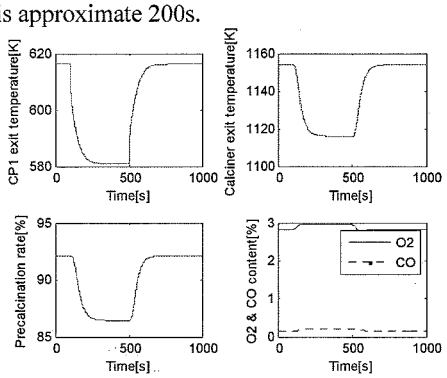

Figure 4. Simulation of step response in raw meal flow rate (+10% at 100s) and (-10% at 500s)

4.2 Change in The $CaCO_3$ Content of Raw Meal

The $CaCO_3$ content of raw meal is other important disturbance variable. An increase of magnitude +10% has been introduced and also again given its initial value at

the 500s. The process response is shown in Fig. 5. As can be appreciated, the CP1 exit temperature, the calciner exit temperature and the precalcination rate all have a decrease, whereas the O_2 content has an increase.

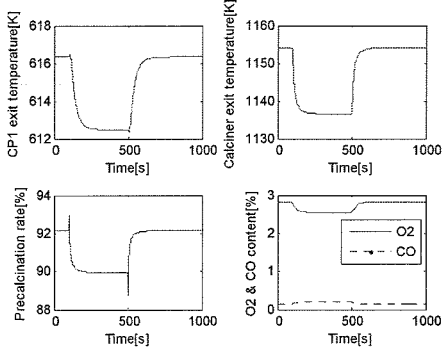

Figure 5. Simulation of step response in raw meal $CaCO_3$ content (+10% at 100s) and (-10% at 500s)

4.3 Change in The Mass Flow Rate of Pulverized Coal

The mass flow rate of pulverized coal is the mainly manipulated variable. The used step change was also +10% of nominal conditions, and again returned to the initial value after the new steady state reached. The process response is shown in Fig. 6. As can be seen, a considerable increase of the CP1 exit temperature, the calciner exit temperature and the precalcination rate is observed. But the O_2 content has an appreciable decrease. The required time to reach the new steady-state operating point is approximate 120s.

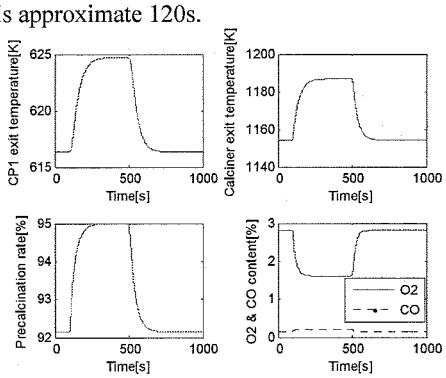

Figure 6. Simulation of step response in coal flow rate (+10% at 100s) and (-10% at 500s)

4.4 Change in The Mass Flow Rate of Tertiary Air

Because there is a strongly coupling relationship between the tertiary air and the gas into rotary kiln, the tertiary air flow rate is not often adjusted. Here a step change of magnitude + 10% was also applied to the tertiary air flow rate in order to obtain the dynamic response. Fig. 7 shows that the calciner exit temperature and the precalcination rate both have a modest decrease and the O_2 content has an increase.

These figures show that the precalciner system is faster to return to a steady state solution given a change in the coal flow rate compared to changes in the flow rate of raw meal. The figure also reveals that the coupling relationship of gas flow rate gives a complex change of the precalciner system.

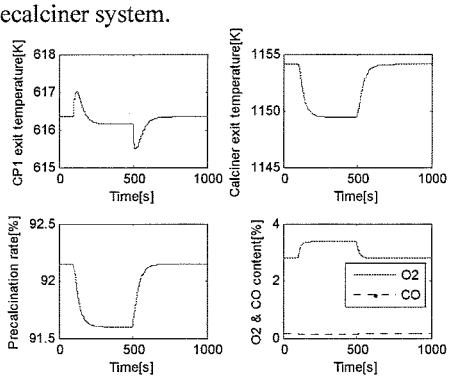

Figure 7. Simulation of step response in tertiary air flow rate (+10% at 100s) and (-10% at 500s)

This is the reason why the tertiary air flow rate was not often adjusted alone. As can be observed, when the O_2 content in the calciner is sufficient, further more increasement to gas flow rate will bring more heat lost from the precalciner system and the CO content has little change.

5. Conclusion

A dynamic first principle model for the cement precalciner system has been developed and presented. It consists of a preheater model and a calciner model. They are both a set of ordinary differential equations for the mass and energy balance.

The static solutions of the model are validated to the hot experimental data, and the precision is satisfactory. The dynamic responses show that changes in the pulverized coal flow rate can control the calciner exit temperature and the precalcination rate while only changes in the tertiary air will cause the whole system complicated changes. The response is similar compared to the operation rules.

The model has not yet been validated on the dynamic experimental data, and the results of dynamic response are only qualitative. The further work has to be done to obtain the quantitative results of dynamic response. But the dynamic model has shown potential to predict the dynamic behavior of the real cement precalciner system.

Acknowledgements

This work was supported by the National High Technology Research and Development Program of China (863 program) (2006AA04Z185).

References

[1] F. Mintus, S. Hamel, & W. Krumm, Wet process rotary kilns: modeling and simulation, *Clean Technologies and Environmental Policy, 8*(2), 2006, 112-122.

[2] Q. D. Chen, *The principle and application of new dry cement technique* (Beijing: China Building Material Industry Publishing House, 2004).

[3] F. N. Koumboulis, & N. D. Kouvakas, Indirect adaptive neural control for precalcination in cement plants, *Mathematics and Computers in Simulation, 60*(3-5), 2002, 325-334.

[4] J. Zou, Y.C.Yang, & J. Zhu, Design of grey model based predictive controllers and its application, *Proceedings of The CSEE, 22*(9), 2002, 12-14.

[5] J. Zou, & J. Zhu, Fuzzy predictive functional control strategy for decomposing furnace temperature system of cement rotary kiln, *Journal of The Chinese Ceramic Society, 29*(4), 2001, 318-321.

[6] D. Xu, & J. Zhu, On calciner temperature control algorithm and realization for cement work with wet grinding and dry-burning, *Journal of The Chinese Ceramic Society, 29*(2), 2001, 119-122.

[7] D. K. Fidaros, C. A. Baxevanou, C. D. Dritselis, & N. S. Vlachos, Numerical modelling of flow and transport processes in a calciner for cement production, *Powder Technology, 171*(2), 2007, 81-95.

[8] K. S. Mujumdar, K. V. Ganesh, S. B. Kulkarni, & V. V. Ranade, Rotary Cement Kiln Simulator (RoCKS): Integrated modeling of pre-heater, calciner, kiln and clinker cooler, *Chemical Engineering Science, 62*(9), 2007, 2590-2607.

[9] K. S. Mujumdar, A. Arora, & V. V. Ranade, Modeling of Rotary Cement Kilns: Applications to Reduction in Energy Consumption, *Industrial and Engineering Chemistry Research, 45*(7), 2006, 2315-2330.

[10] L. Wan, & C. Yang, *Modeling and Simulation for 440t/h CFB Boiler Air-Flue Gas System* (Chongqing: Chongqing University, 2005).

Appendix

Nomenclature	
E	activation energy
M	mole mass
R	perfect-gas constant
T	temperature
V	volume
$\triangle H$	reaction heat
c	specific heat
f	flow rate
k	preexponential factor
m	mass
p	percentage
r	specific reaction rate
Greek symbol	
η	separate efficiency
Subscripts	
Al_2O_3	alumina
C	carbon
$CaCO_3$	calcium carbonate
CaO	calcium oxide
CO	carbon monoxide
CO_2	carbon dioxide
Fe_2O_3	ferric oxide
O_2	oxygen
cal	calciner
d	dust
g	gas
i	the stage of preheater
ke	kiln exhaust
s	solid
ta	tertiary air